Int. J. Radiation Oncology Biol. Phys., Vol. 67, No. 4, pp. 1187–1200, 2007

0360-3016/07/$–see front matter

ELSEVIER

doi:10.1016/j.ijrobp.2006.11.040

BIOLOGY CONTRIBUTION

ESTROGENS DECREASE γ-RAY–INDUCED SENESCENCE AND MAINTAIN CELL CYCLE PROGRESSION IN BREAST CANCER CELLS INDEPENDENTLY OF p53

Robert-Alain Toillon, Ph.D.,* Nicolas Magné, M.D., Ph.D.,† Ioanna Laïos, B.Sc.,* Pierre Castadot, M.D.,† Eric Kinnaert, Ph.D.,† Paul Van Houtte, M.D.,† Christine Desmedt, B.Sc.,‡ Guy Leclercq, Ph.D.,* and Marc Lacroix, B.Sc.*

*Laboratoire Jean-Claude Heuson de Cancérologie Mammaire, Université Libre de Bruxelles, Brussels, Belgium; †Radiotherapy Unit and ‡Microarray Unit, Institut Jules Bordet, Brussels, Belgium

Purpose: Sequential administration of radiotherapy and endocrine therapy is considered to be a standard adjuvant treatment of breast cancer. Recent clinical reports suggest that radiotherapy could be more efficient in association with endocrine therapy. The aim of this study was to evaluate the estrogen effects on irradiated breast cancer cells (IR-cells).

Methods and Materials: Using functional genomic analysis, we examined the effects of 17-β-estradiol (E_2, a natural estrogen) on MCF-7 breast cancer cells.

Results: Our results showed that E_2 sustained the growth of IR-cells. Specifically, estrogens prevented cell cycle blockade induced by γ-rays, and no modification of apoptotic rate was detected. In IR-cells we observed the induction of genes involved in premature senescence and cell cycle progression and investigated the effects of E_2 on the p53/p21$^{waf1/cip1}$/Rb pathways. We found that E_2 did not affect p53 activation but it decreased cyclin E binding to p21$^{waf1/cip1}$ and sustained downstream Rb hyperphosphorylation by functional inactivation of p21$^{waf1/cip1}$. We suggest that Rb inactivation could decrease senescence and allow cell cycle progression in IR-cells.

Conclusion: These results may help to elucidate the molecular mechanism underlying the maintenance of breast cancer cell growth by E_2 after irradiation-induced damage. They also offer clinicians a rational basis for the sequential administration of ionizing radiation and endocrine therapies. © 2007 Elsevier Inc.

Estrogen, Senescence, Breast cancer, Radiation, p53, p21$^{waf1/cip1}$, DNA damage, Rb, Cyclin.

INTRODUCTION

Estrogens are involved in the progression of most breast tumors (1). The biologic effects of estrogens are mediated by their binding to estrogen receptors (ERα or ERβ). Nevertheless, in breast cancer, ERα is predominant and the β-form is down-regulated (2, 3). The ERs are well known as ligand-dependent transcription factors. In addition, they increasingly appear to engage in cross-talk with growth factors signaling pathways independently of the transcriptional activity (4). Endocrine therapy is of major importance in the adjuvant treatment of breast cancer. However, endocrine therapy is generally associated with radiotherapy, and few experimental and/or clinical studies are available regarding the combined effects of both therapies (5).

Therefore, we designed *in vitro* experiments to determine the impact of estrogens on breast cancer cell (BCC) response to γ-ray irradiation. We have previously reported that estrogens decreased radiosensitivity of MCF-7 BCC (6). Direct and indirect actions of estrogens on target genes might explain this effect. For instance, the cross-talk between estrogen and growth factor transduction cascades, including the MAP-kinase and PI3-kinase pathways (7, 8), may potentially inhibit the effects of ionizing radiation (9). Direct estrogen effects through activated ERα activation with specific promoter sequences might also be involved in radioresistance. In particular, estrogens may induce cyclin D1 and c-myc expression, allowing cell cycle progression via cyclin/cdk activation and subsequent G_1/S and G_2/M transitions (10).

Reprint requests to: Robert-Alain Toillon, Ph.D., ERI-8 INSERM, Université des Sciences et Technologies de Lille, Bâtiment SN3, 59655 Villeneuve d'Ascq, France. Tel: (+33) 3-20-43-40-37; Fax: (+33) 3-20-47-40-38; E-mail: robert.toillon@univ-lille1.fr

Robert-Alan Toillon, Ph.D., and Nicolas Magné, M.D., contributed equally to this work.

Supported by grants from les Amis de l'Institut Bordet, and by the Fonds National de la Recherche Scientifique (to R.-A.T. and C.D.).

Conflict of interest: none.

Acknowledgments—The authors thank H. Duvillier and N. Jouy for flow cytometry analysis and J. Richard for secretarial assistance.

Received Dec 29, 2005, and in revised form Oct 19, 2006. Accepted for publication Nov 20, 2006.

Other hypotheses have been suggested to explain the effects of estrogen on radiosensitivity, including inactivation of p53 (11).

Based on these hypotheses and experimental data, we dissected the functional mechanisms underlying estrogen effects on BCC exposed to γ-rays, using MCF-7 cells as a model of hormone-dependent, p53 wild-type breast cancer cells (12).

METHODS AND MATERIALS

Cell culture

The MCF-7 BCC were routinely grown in basal Eagle's minimal essential medium (EMEM) supplemented with 10% inactivated fetal calf serum (FCS), 100 UI/ml streptomycin and 100 μg/ml penicillin. For experiments, cells were cultured in basal EMEM without phenol red and supplemented with 10% inactivated and charcoal-dextran–stripped FCS.

Reagents and antibodies

All cell culture reagents were from Life Technologies (Rockville, MD). Electrophoresis reagents and agarose bound antibodies were obtained from Sigma (Bornem, Belgium). Mouse monoclonal and rabbit polyclonal anti-$p21^{waf1/cip1}$, anti-p53, cyclin A, cyclin D1, cyclin E2, Rb antibodies were from Cell Signaling (Beverly, MA), mouse monoclonal anti-$p27^{kip1}$ antibody was provided by Novocastra (Zaventem, Belgium). Horseradish peroxidase–conjugated secondary antibodies were from Pierce (Erembodegem, Belgium). Pharmacologic inhibitors were from Calbiochem (Leuven, Belgium).

Ionizing radiation conditions

Irradiation was performed 48 h after plating using high-energy photons from a linear accelerator 18 MV (Clinac, Varian Medical Systems) with 4 Gy/min at room temperature. Medium was removed and replaced by fresh medium at the time of irradiation. Cells were maintained in basal EMEM supplemented with 10% inactivated and charcoal-dextran–stripped FCS during all radiation exposures.

Cell growth assays

Viable cell growth assay. Cells were gently washed once with phosphate-buffered saline (PBS), fixed with 1% glutaraldehyde/PBS (15 min, 20°C) and stained with 0.1% crystal violet (w/v in ddH_2O) (30 min, 20°C). Excess of crystal violet dye was then removed by three washes of running tap water (15 min, 20°C) and cells were lysed with 0.2% Triton X-100 (v/v in ddH_2O) (90 min, 20°C, under agitation). The absorbance was measured at 550 nm using a Microplate Autoreader EL309 (BIO-TEK Instruments, Winooski, VT).

Clonogenic assays. Clonogenic assays were performed as previously described (13). Briefly, MCF-7 cells were plated at a density of 25,000/dish in 35-mm dishes and cultured in basal EMEM without phenol red and supplemented with 10% inactivated and charcoal-dextran–stripped FCS. The bottom layer was prepared with 0.56% Bacto agar. Cells were seeded over the bottom layer in 0.37% Bacto agar containing medium. Cells were allowed to grow for 10 or 21 days before colonies of at least 20 or 50 cells were counted, respectively. Survival was fitted to the linear-quadratic model $S = e^{-(\alpha D + \beta D^2)}$.

Cell cycle analysis. MCF-7 cells were maintained 48 h in estrogen free medium before treatment. At the end of the experiment cells were trypsinized and washed twice with PBS. They were subsequently stained by Cell Cycle Coulter reagent (Beckman Coulter, Co., Fullerton, CA). Briefly, pelleted cells (1×10^6) were mixed thoroughly with 50 μl of reagent A (15 s, 20°C, under vortex agitation) and 950 μl of reagent B. After incubation (2 h, 4°C, dark), the cell cycle was analyzed with a Beckman Facs analyzer.

Senescence-associated β-galactosidase staining. Staining was performed as previously described (14). Four days after ionizing radiation, cells were washed twice and fixed with 3% paraformaldehyde, pH 7.2. Cells were then washed and stained with a solution of 1 mg/ml 5-bromo-4-chloro-indolyl-B-galactoside (X-Gal, Sigma) [pH 6], in 5 mmol/L potassium ferrocyanide, 5 mmol/L potassium ferricyanide, 150 mmol/L NaCl, 40 mmol/L citric acid, and 2 mmol/L $MgCl_2$ (37°C, 24 h). After incubation, cells were washed twice with PBS and stained for SA–β-galactosidase assessment under light microscopy.

Microarray analysis

Total RNA was isolated from the cells (TRIzol reagent; Gibco BRL Life Technologies, Rockville, MD), and purified using RNeasy (Qiagen, Valencia, CA). cRNA was prepared exactly as described by the microarray manufacturer (Affymetrix, Santa Clara, CA). The concentration and the integrity/purity of each RNA sample were measured using RNA 6000 LabChip kit (Agilent Technologies, Palo Alto, CA) and an Agilent 2100 bioanalyzer. A 3-μg quantity of total RNA was used for the preparation of double-stranded cDNA using an oligo $(dT)_{24}$ primer with a T7 RNA polymerase promoter sequence at its 5′ end. After second strand synthesis, a labeled cRNA transcript was generated from the cDNA in an *in vitro* transcription reaction using Enzo BioArray high yield RNA transcript labeling (Enzo Diagnostics, Inc., Farmingdale, NY). The labeled anti-sense RNA was purified using RNeasy and each cRNA sample (20 μg) was fragmented (94°C, 35 min). The DNA microarrays used in this study were the U133 Plus 2.0 Array (Affymetrix, Santa Clara, CA), containing almost 47,000 probe sets. Each probe set consisted of 22 different oligonucleotides (11 of which are a perfect match with the target transcript and 11 of which harbor a single-nucleotide mismatch in the middle). These 22 oligonucleotides were used to measure the level of a given transcript. Details of the RNA amplification, labeling, and hybridization steps are available at http://www.affymetrix.com. Chips were scanned, and background correction, normalization, and summarization of the data were done using the robust multi-array average procedure (15).

Cellular extract

Total extract. Cell cultures were washed with PBS and lysed for 30 min at 4°C in lysis buffer (50 mmol/L Tris [pH 7.5], 150 mmol/L NaCl, 1% Igepal, 0.1% SDS, 0.5% sodium deoxycholate, 50 mmol/L NaF, 0.6 mmol/L PMSF, 0.1 mmol/L orthovanadate, and 0.3 mmol/L TPCK). After centrifugation (15 min, 4°C, 16,000 *g*), the supernatants were collected as total extract.

Cytoplasmic and nuclear extracts. For the extracts, 2.5×10^6 cells were washed twice with ice-cold PBS and lysed in hypotonic buffer (10 mmol/L 4-(2-Hydroxyethyl) piperazin-1-ethanesulphonic acid [HEPES] [pH 7.9], 1.5 mmol/L $MgCl_2$, 10 mmol/L KCl, 2 mmol/L Na_3VO_4, 0.2 mmol/L phenylmethylsulphonyl fluoride (PMSF), 3 μg/ml aprotinin, 25 μg/ml pepstatin, 25 μg/ml leupeptin, 25 μg/ml chymotrypsin, 5 mmol/L NaF, 0.5 mmol/L dithiothreitol (DTT), 0.1% Igepal). After centrifugation (5 min,

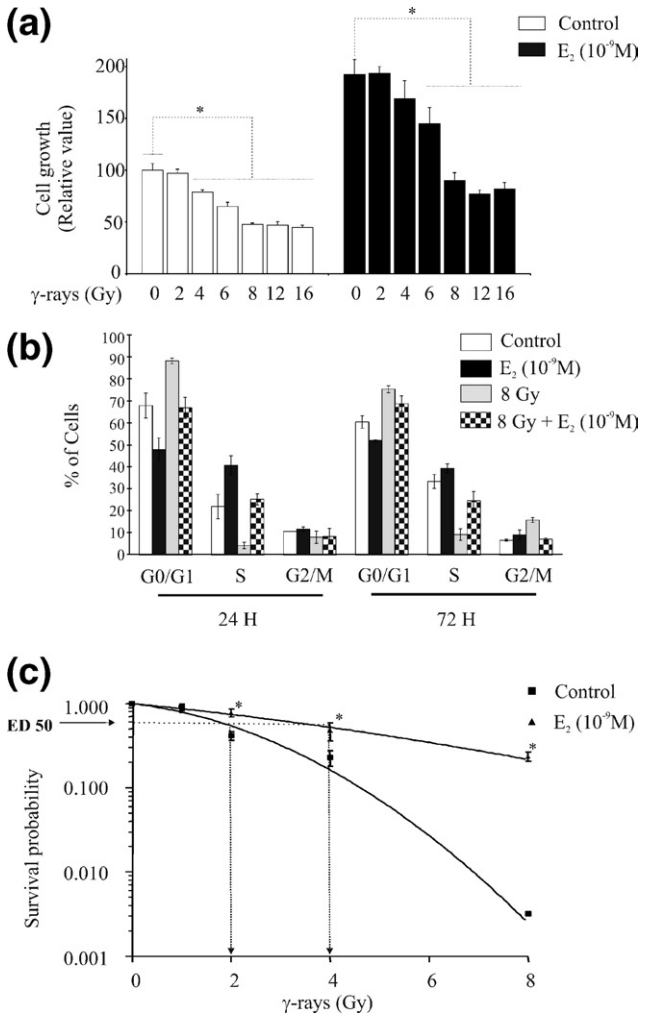

Fig. 1. Effects of E_2 on irradiated breast cancer cells (IR-cells) growth. (a) MCF-7 viable cell growth was assessed by crystal violet staining 96 h after γ-rays ionizing radiation exposure (0–16 Gy) in the absence or presence of 10^{-9} mol/L of 17-β-estradiol (E_2). (b) Flow-cytometric analysis of cell cycle distribution in IR-cells 24 and 72 h postirradiation at the 8-Gy γ-ray dose. (c) Clonogenic survival at Day 10 of MCF-7 cells upon γ-ray exposure (0–8 Gy), the experimental results are fitted to the linear-quadratic model. Results are representative of three independent experiments performed in triplicate assays. $*p < 0.05$.

4°C, 16, 000 g), the supernatants were collected as cytosol. Nuclear extracts were prepared by resuspension of the crude nuclei in high salt buffer (20 mmol/L HEPES [pH 7.9], 1.5 mmol/L $MgCl_2$, 420 mmol/L NaCl, 2 mmol/L Na_3VO_4, 0.2 mmol/L PMSF, 3 μg/ml aprotinin, 25 μg/ml pepstatin, 25 μg/ml leupeptin, 25 μg/ml chymotrypsin, 5 mmol/L NaF, 0.5 mmol/L DTT, 25% glycerol) (10 min, 4°C). The nucleoprotein-containing supernatants were collected after centrifugation (5 min, 4°C, 16,000 *g*) and conserved at −70°C until use.

Active p53 ELISA

At the end of experiment, 20 μg of nuclear extracts were used to measure p53 DNA-binding ability using a DuoSet IC active p53 ELISA kit as described by the manufacturer (R&D Systems, Abingdon, UK; www.RnDSystems.com).

Western blot

Western blots were performed as previously described (6). Blots were incubated with primary antibody (1:1,000 dilution, overnight at 4°C). Detection was performed using a goat anti-mouse secondary antibody or goat anti-rabbit secondary antibody (1:2,000 dilution, 1.5 h at room temperature) and Western Pico Detection system (Pierce, Erembodegem, Belgium).

Immunoprecipitation

Cells were washed with PBS and lysed for 30 min at 4°C in lysis buffer (50 mmol/L Tris [pH 7.5], 150 mmol/L NaCl, 1% Igepal, 1 mmol/L PMSF, 1 mmol/L orthovanadate, 1 mmol/L $Na_4P_2O_7$, 10 mg/ml aprotinin, and 10 mg/ml leupeptin). Lysates were cleared by centrifugation (12,000 *g,* 10 min). A 1-mg quantity of cellular extracts was pre-cleared with 5 μl protein A/G PLUS-Agarose (2 h, 4°C) and incubated with primary antibody (2 μg, overnight at

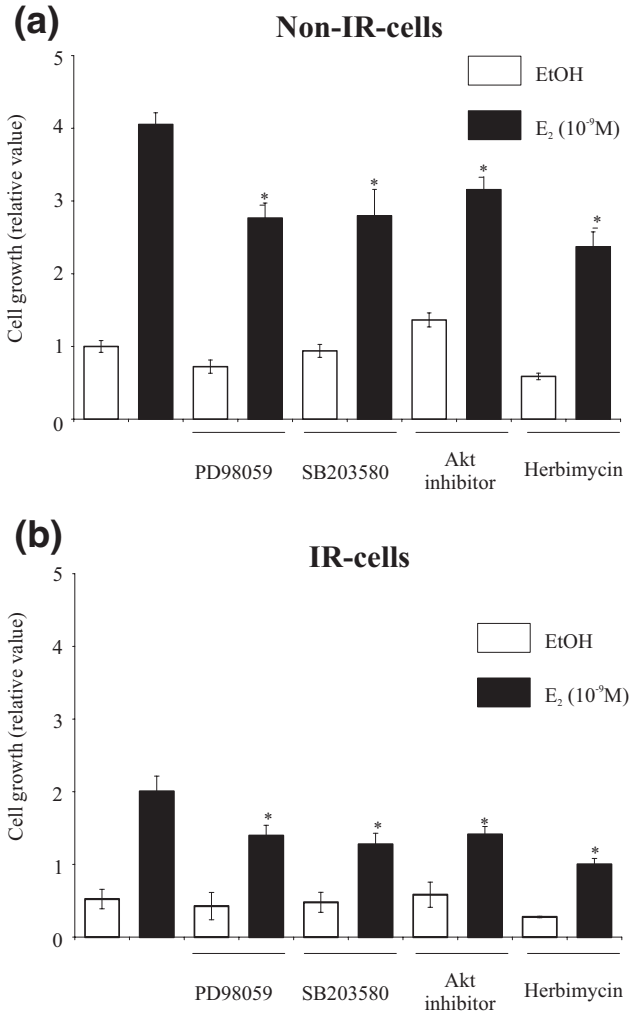

Fig. 2. Influence of pharmacologic inhibitors of growth factors transduction pathways on the estrogen receptor–α (ERα) rescue effects on cells growth. At 96 h postirradiation, viable cell growth was appreciated by crystal violet staining in presence of different combination of E_2 (10^{-9} mol/L) and pharmacologic inhibitors of MAP-kinase (PD98059, 10 μmol/L), P38 MAP-kinase (SB 203580, 5 μmol/L), Akt (Akt inhibitor, 5 μmol/L), and src (herbimycin, 100 nmol/L). Results are representative of three independent experiments performed in triplicate assays. $*p < 0.05$.

Table 1. Microarray analysis of effects of E_2 on γ-ray–modulated genes

Accession number	Gene name (Symbol)	Fold change (control = 1) 8 Gy	E_2	8 Gy + E_2	Pathways
NM_001107	ACYP1	0.46	1.94	1.68	
AI744123	ANKRD43	0.48	0.46	0.27	
NM_018685	ANLN	0.35	2.33	0.81	E2F
NM_030920	ANP32E	0.36	2.78	1.24	
NM_001159	AOX1	0.49	0.29	0.45	
NM_004900	APOBEC3B	0.36	0.50	0.32	
NM_018154	ASF1B	0.44	2.66	1.34	
NM_018123	ASPM	0.35	1.55	2.36	
AI925583	ATAD2	0.44	2.29	1.12	ER
AB011446	AURKB	0.41	2.75	1.08	E2F
BE672260	B3GNT5	0.46	0.51	0.25	
AA648913	BIRC5	0.46	2.15	1.07	p53/E2F
NM_000059	BRCA2	0.46	2.37	0.95	E2F
D38553	BRRN1	0.38	2.48	1.08	E2F
AF043294	BUB1	0.33	2.21	0.97	E2F
NM_001211	BUB1B	0.43	2.23	1.02	E2F
NM_018131	C10orf3	0.27	0.79	0.87	
BF792864	C15orf23	0.41	2.14	1.21	
BC001068	C20orf129	0.39	2.00	1.17	
NM_024053	C22orf18	0.44	1.89	0.95	
BG492359	C6orf173	0.48	3.00	1.35	
BF248364	CASC5	0.33	2.02	0.83	
R60224	CBLN2	0.41	0.34	0.22	
NM_001237	CCNA2	0.26	2.51	1.08	E2F
N90191	CCNB1	0.37	1.53	0.76	E2F
NM_004701	CCNB2	0.35	1.74	0.91	E2F
NM_001786	CDC2	0.41	1.53	0.83	E2F
NM_001255	CDC20	0.35	2.63	1.33	E2F
NM_001790	CDC25C	0.25	1.66	0.61	E2F
NM_003504	CDC45L	0.49	4.96	2.07	E2F
NM_001254	CDC6	0.39	4.23	1.82	E2F
AF326731	CDCA1	0.34	2.88	0.86	
T90295	CDCA2	0.40	1.98	1.20	
NM_031299	CDCA3	0.35	2.2	1.05	
BE614410	CDCA5	0.44	3.33	1.80	
AY029179	CDCA7	0.39	7.87	2.60	
BC001651	CDCA8	0.44	2.21	1.24	
NM_001262	CDKN2C	0.30	1.38	0.73	E2F
AF213040	CDKN3	0.31	1.99	1.06	E2F
AW075105	CDT1	0.43	3.29	1.43	E2F
NM_001809	CENPA	0.30	2.23	0.97	E2F
NM_001813	CENPE	0.40	2.19	3.70	E2F
NM_005196	CENPF	0.39	1.26	1.14	E2F
AL572471	CENPH	0.43	1.86	0.86	E2F
AI861788	CIT	0.48	1.45	2.17	
NM_001827	CKS2	0.46	1.98	1.18	E2F
AA406603	CLCC1	0.47	1.54	2.38	
NM_024094	DCC1	0.38	3.87	1.86	
NM_017779	DEPDC1	0.26	3.05	1.10	
AK001166	DEPDC1B	0.35	2.43	1.04	
NM_000791	DHFR	0.47	2.31	1.14	E2F
NM_014750	DLG7	0.31	1.91	0.82	
NM_016448	DTL	0.43	6.40	2.73	
AI341146	E2F7	0.47	5.66	2.07	E2F
NM_024680	E2F8	0.31	2.97	1.18	
NM_018098	ECT2	0.43	1.39	1.47	
BC040700	EP300	0.44	2.03	1.55	
NM_012291	ESPL1	0.37	1.66	0.78	E2F
NM_003686	EXO1	0.42	3.96	1.85	E2F
AI346350	EXOSC9	0.34	2.71	0.93	
AL512760	FADS1	0.50	1.39	1.01	
AL138828	FAM54A	0.46	3.15	1.66	

Continued

Table 1. Microarray analysis of effects of E_2 on γ-ray–modulated genes (*Continued*)

Accession number	Gene name (Symbol)	Fold change (control = 1)			Pathways
		8 Gy	E_2	8 Gy + E_2	
BC005004	FAM64A	0.46	2.30	1.18	
NM_012177	FBXO5	0.46	2.65	1.10	
NM_021953	FOXM1	0.41	1.97	3.88	
NM_006733	FSHPRH1	0.39	2.10	0.96	
AY028916	GAJ	0.36	6.04	1.88	
H37811	GAS2L3	0.41	1.67	0.91	
NM_016426	GTSE1	0.28	1.48	0.71	E2F
NM_022346	HCAP-G	0.28	3.82	1.43	
AI650364	HELLS	0.50	2.92	1.35	
BC000903	HMGB2	0.30	1.70	0.71	E2F
NM_012485	HMMR	0.26	2.00	0.73	
AW271106	IQGAP3	0.46	1.30	1.82	
NM_014736	KIAA0101	0.30	1.67	0.87	
NM_004523	KIF11	0.36	1.91	3.47	
NM_014875	KIF14	0.24	1.89	0.71	
NM_020242	KIF15	0.20	2.39	0.70	
NM_031217	KIF18A	0.44	1.91	3.34	
NM_005733	KIF20A	0.34	1.72	0.83	E2F
NM_004856	KIF23	0.29	1.47	0.68	E2F
U63743	KIF2C	0.30	2.10	1.04	E2F
NM_012310	KIF4A	0.32	1.67	0.79	E2F
BC000712	KIFC1	0.45	1.93	1.19	
NM_006101	KNTC2	0.31	2.10	0.96	E2F
NM_005573	LMNB1	0.29	2.33	0.83	
NM_017760	LUZP5	0.40	2.47	1.11	
NM_002358	MAD2L1	0.33	3.10	1.57	E2F
NM_018518	MCM10	0.35	5.87	2.51	E2F
NM_014791	MELK	0.41	2.32	1.12	E2F
AI871282	MGC70924	0.49	1.23	1.01	
AU147044	MKI67	0.30	1.91	0.64	E2F
NM_024629	MLF1IP	0.42	2.33	1.20	
NM_012329	MMD	0.41	2.09	0.99	
NM_002466	MYBL2	0.43	1.71	0.90	E2F
NM_018248	NEIL3	0.36	4.06	1.16	E2F
NM_002497	NEK2	0.31	1.71	0.77	E2F
NM_006681	NMU	0.42	5.15	2.11	
NM_002452	NUDT1	0.49	2.07	1.14	
NM_018454	NUSAP1	0.33	1.89	0.76	
BE045993	OIP5	0.44	2.70	1.19	
AI934557	PAQR5	0.39	0.65	0.68	
NM_018492	PBK	0.31	3.24	1.42	
NM_014264	PLK4	0.37	2.03	0.79	E2F/ER
NM_002692	POLE2	0.44	1.87	3.72	E2F
NM_003981	PRC1	0.34	2.19	0.97	E2F
NM_004219	PTTG1	0.34	1.84	0.91	E2F
AU153848	RACGAP1	0.41	1.47	0.82	E2F
BE966146	RAD51AP1	0.30	2.69	1.19	E2F
AB051846	RAP1A	0.17	0.24	0.22	E2F
BE966236	RRM2	0.30	3.78	2.00	E2F
AF116616	SCD	0.48	2.54	1.61	E2F
N31731	SGOL2	0.42	2.05	1.03	
NM_024745	SHCBP1	0.38	3.37	1.60	
NM_003035	SIL	0.48	2.01	1.05	
NM_005496	SMC4L1	0.49	1.73	3.00	E2F
NM_006461	SPAG5	0.40	2.40	1.10	
AF225416	SPBC25	0.37	2.23	0.82	
NM_003600	STK6	0.44	1.88	1.18	
NM_006342	TACC3	0.34	2.12	1.17	
BC002493	TCF19	0.43	2.19	1.17	E2F
NM_003258	TK1	0.47	1.73	1.03	E2F
BF338045	TNFAIP8L1	0.38	1.37	0.83	
AL561834	TOP2A	0.33	1.54	0.76	E2F

Continued

Table 1. Microarray analysis of effects of E_2 on γ-ray–modulated genes (*Continued*)

Accession number	Gene name (Symbol)	Fold change (control = 1) 8 Gy	E_2	8 Gy + E_2	Pathways
AF098158	TPX2	0.43	1.22	1.83	E2F
NM_004237	TRIP13	0.48	3.36	1.58	
NM_005480	TROAP	0.36	1.46	2.90	
NM_003318	TTK	0.27	2.19	0.97	E2F
NM_007019	UBE2C	0.32	1.73	0.91	E2F
AK025578	UHRF1	0.35	2.69	1.21	
AW772140	WDHD1	0.49	2.47	5.80	
NM_014950	ZBTB1	0.48	0.65	0.66	
N62196	ZNF367	0.38	4.30	2.15	
NM_007057	ZWINT	0.49	1.93	1.09	E2F
NM_001613	ACTA2	4.34	1.07	0.62	
NM_000700	ANXA1	2.23	0.94	1.19	
AW151108	ATRNL1	2.19	1.31	1.62	
NM_004324	BAX	2.22	1.22	0.84	p53
AI827789	BCMP11	2.04	1.24	1.25	
NM_006763	BTG2	2.71	0.58	0.90	p53/E2F
NM_001584	C11orf8	2.13	14.96	5.28	ER
NM_020375	C12orf5	2.19	1.19	1.24	p53
NM_020215	C14orf132	2.12	0.13	0.29	
NM_001753	CAV1	2.10	0.48	0.18	p53/senescence
BE903880	CD44	2.09	6.14	0.45	senescence
AW274756	CDK6	2.17	0.16	0.09	E2F
NM_000389	CDKN1A	3.65	0.66	1.06	p53/E2F
AF317887	Cep290	2.10	0.94	1.06	
AF101051	CLDN1	2.78	0.26	0.16	senescence
NM_001338	CXADR	2.06	2.58	0.99	
NM_000499	CYP1A1	2.48	0.42	0.24	
AU154504	CYP1B1	2.33	0.88	1.13	
NM_000107	DDB2	2.19	1.65	1.02	p53
U46745	DTNA	2.19	0.80	0.73	
NM_001394	DUSP4	2.75	2.51	2.32	
T15545	EPHA4	2.02	1.99	0.41	
NM_000043	FAS	6.15	2.08	1.04	p53
AK024690	FBXL20	2.15	0.89	0.50	
AA129444	FSTL5	2.88	0.63	0.26	
AF180519	GABARAPL3	2.21	0.46	0.33	
NM_001924	GADD45A	2.96	1.34	1.49	p53
AF003934	GDF15	6.12	1.76	2.16	p53
BM668595	GPATC2	2.01	0.30	0.24	
NM_002510	GPNMB	2.72	0.86	1.48	
BE675337	GSN	2.03	0.64	0.68	
AW731710	HINT3	2.13	0.59	0.57	
NM_003543	HIST1H4H	2.06	0.42	1.18	Senescence
M16276	HLA-DQB1	2.29	0.49	0.53	Myc/ER
NM_016545	IER5	2.18	2.00	1.36	
BM128432	IGFBP5	2.05	1.63	1.88	
AJ007557	KCNJ13	2.65	0.72	0.25	
U11058	KCNMA1	2.06	0.49	0.36	
NM_014732	KIAA0513	2.01	0.24	0.37	
NM_025081	KIAA1305	2.57	0.99	0.38	
NM_005780	LHFP	2.22	0.29	0.13	
AI375083	LRFN5	2.04	0.86	0.33	
NM_024548	LRRIQ2	2.26	2.65	0.85	
NM_005360	MAF	2.16	0.79	0.50	p53
NM_005757	MBNL2	2.09	0.87	0.48	
AJ276888	MDM2	2.22	1.73	1.53	p53
AF278532	NTN4	2.56	0.18	0.14	
NM_020190	OLFML3	2.18	0.52	1.30	
AI806586	OSBPL9	2.05	037	0.29	
AI524125	PCDH9	2.03	0.96	0.64	
AW968465	PGM5P1	2.01	0.63	0.33	
BF589462	PPM1L	2.18	0.96	0.57	

Continued

Table 1. Microarray analysis of effects of E_2 on γ-ray–modulated genes (*Continued*)

Accession number	Gene name (Symbol)	Fold change (control = 1)			Pathways
		8 Gy	E_2	8 Gy + E_2	
BG285881	PRICKLE2	2.15	0.66	0.60	
AW471145	PRSS23	2.42	4.87	1.11	ER/senescence
AW242315	PTGER3	2.46	0.37	0.24	
BC040303	PTP4A1	2.34	0.77	0.61	
BC003667	RPS27L	2.90	1.21	0.79	
NM_016656	RRAGB	2.09	0.59	0.51	
NM_002615	SERPIFN1	2.58	1.29	0.95	
AA488687	SLC7A11	2.71	32.11	4.31	
AI559300	SPATA18	5.08	1.07	0.70	
NM_001062	TCN1	3.25	72.41	63.46	
AV660825	TMEM49	2.31	0.32	0.22	
NM_014058	TMPRSS11E	2.83	0.53	0.32	
AF016266	TNFRSF10B	2.58	1.34	1.18	p53
NM_016629	TNFRSF21	2.01	2.33	1.18	
AW341649	Tp53INP1	2.83	0.08	0.30	p53
AW024437	TTC18	2.19	0.78	0.38	
L22431	VLDLR	3.04	2.95	0.69	
NM_022470	WIG1	3.85	0.48	0.55	p53

4°C, on rotating device). Immune complex was then collected after incubation with 25 μl of protein A/G PLUS-Agarose (2 h, 4°C, on rotating device) and centrifugation (12,000 *g*, 3 min). Immunoprecipitates were washed three times with ice-cold lysis buffer and analyzed by Western blot as previously described.

Statistical analysis

Statistical significance was measured by Student's paired *t* test. A value of $p < 0.05$ was considered statistically significant.

RESULTS

E_2 prevented cell growth inhibitory effects of γ-rays on MCF-7 BCC

As shown in Fig. 1a, a dose-dependent decrease in MCF-7 cell growth was observed in irradiated breast cancer cells (IR-cells) up to 8 Gy, higher doses did not provoke further inhibition of cell growth. Our findings showed that E_2 sustained cell growth in IR-cells independently of the radiation doses. Therefore, cell cycle parameters were assessed at 8 Gy (Fig. 1b). In non-IR cells, E_2 rapidly induced cell proliferation (50% of cells in S and G2/M phases after 24 h) and maintained it at 72 h. In IR-cells, cell proliferation was stopped at 24 h (90% of cells in G0/G1-phase). A slight decrease in G0/G1 and an increase in G2/M were observed at 72 h, indicating that some cells bypassed the initial G0/G1 arrest but were then blocked in G2/M. Treatment with E_2 prevented cell cycle arrest in IR-cells. Confirming our previous report (6), no significant modification of apoptosis induction was associated with IR-cell cycle blockade either in the absence or in the presence of E_2 (data not shown).

The cell growth studies were substantiated by assessment of clonogenic survival at 10 and 21 days after γ-rays exposure. The γ-ray exposure reduced survival of MCF-7 cells after 10 days (Fig. 1c) and 21 days (data not shown). After 10 days the efficient dose to observe 50% of growth inhibition (ED-50) value was lower than in the monolayer culture condition and was evaluated to 2 Gy, corresponding to the relevant clinical dose. In these conditions, E_2 clearly decreased radio-sensitivity, increasing the ED-50 value to 4 Gy.

E_2-induced radio-resistance did not require cross-talk with growth factor pathways

To assess whether cross-talk with growth factor pathways was involved in E_2-induced cell growth rescue, various pharmacologic inhibitors of these pathways were used (Fig. 2). All inhibitors partly decreased E_2-induced cell growth in both non–IR-cells and IR-cells. However, none was able to abolish the rescue effect of E_2 on IR-cell growth.

Gene expression analysis of E_2-induced radio-resistance genes

Microarray analysis was performed to investigate gene modulation by E_2 in IR-cells (Tables 1 and 2). In all, 312 probe sets were found to be differentially modulated (at least 2-fold increase or decrease) upon γ-ray exposure corresponding to 204 genes (Table 1) Among these genes, 108 were relevant to cell growth. Comparing our data with those of previous studies, we determined that the majority of cell growth-associated genes modulated by 8 Gy γ-rays (79 genes) were related to p53 activation (15 genes) (16), induction of senescence (5 genes) (17–19), and/or inhibition of E2F (61 genes) (20) (Table 1). In IR-cells, E_2 treatment clearly down-regulated the induction of senescence-associated gene (*CDLN1, CAV1, HIST1H4H, PRSS23*, *CD44*) and up-regulated E2F-target genes (Table 1). We found that E_2 did not significantly modify the expression of the major p53-

Table 2. Microarray analysis of γ-ray modulation of E_2-dependent genes

Accession number	Gene name (Symbol)	Fold change (control = 1)			Pathways
		8 Gy	E_2	8 Gy + E_2	
AW069729	ACPL2	1.24	1.17	0.59	
N29801	ADAM22	0.98	1.52	0.65	EMT
AW203986	AFTIPHILIN	0.90	1.95	0.74	
AF279145	ANTXR1	0.89	1.56	0.59	
AB011132	AQR	1.03	1.21	0.52	
BG253884	BTBD15	0.87	1.10	0.40	
AI634652	C8orf44	0.99	1.75	0.81	
BF792631	CDC14B	0.83	1.52	0.58	p53
AF317887	Cep290	0.94	2.10	0.84	
AW514564	CHD2	0.98	1.00	0.48	
AF070621	DIXDC1	0.96	1.78	0.78	
NM_001406	EFNB3	0.76	1.30	0.49	EMT
AW138704	FAM76B	1.06	1.27	0.62	
D80480	FLJ14624	0.95	1.14	0.49	
AW975050	FLJ31568	0.88	1.27	0.47	
AI247824	FLJ36665	1.30	1.65	0.79	
AA129444	FSTL5	0.63	2.88	0.75	
AL041745	GPM6B	1.10	1.49	0.63	
BE544748	GSPT1	1.13	1.40	0.59	translation
AK001846	HNRPR	1.17	1.51	0.74	
N95466	HNRPU	1.49	1.66	0.78	
BE466675	IBSP	0.65	1.84	0.57	
M96843	ID2B	0.98	1.77	0.85	EMT
AI743396	KCMF1	1.05	1.19	0.56	
AJ007557	KCNJ13	0.72	2.65	0.69	
NM_025081	KIAA1305	0.99	2.57	1.00	
AA992480	KIDINS220	0.94	1.67	0.72	
NM_014398	LAMP3	1.04	1.47	0.50	p53
AW242720	LOC143381	1.08	1.61	0.79	
AA528080	LOC283070	0.56	1.18	0.32	
AA417117	LOC344595	0.94	3.12	1.25	
BE466160	LOC388526	1.03	2.12	0.89	
AI375083	LRFN5	0.87	2.04	0.67	
AA642143	M11S1	0.86	1.61	0.68	
BE674528	MAF	0.70	3.33	0.77	
NM_018298	MCOLN3	0.81	1.43	0.54	
AI382029	MYO9A	1.11	1.94	0.93	
BE670307	NA	0.68	1.74	0.45	
AU145501	NA	0.79	2.09	0.67	
BE464799	NA	0.84	1.33	0.55	
BF032500	NA	0.98	1.74	0.77	
BE552208	NA	0.95	1.03	0.45	
AW440490	NA	0.96	1.09	0.51	
BC026304	NA	1.92	2.15	1.01	
AU157716	NA	1.05	1.02	0.49	
AW083948	NFYB	0.68	1.23	0.39	senescence
AI743090	NPAS2	0.87	1.98	0.77	
AW003022	NRF1	1.15	1.15	0.52	EMT
AI149508	ORC4L	0.61	1.40	0.28	
AI818048	PHF10	0.93	1.25	0.59	
NM_005044	PRKX	0.95	1.54	0.68	
AL536268	RBMS2	0.91	2.60	1.04	
AI472310	RFP2	0.85	1.34	0.56	
NM_014746	RNF144	0.99	1.08	0.52	
AI694536	SNTB2	0.73	1.45	0.41	
NM_153039	TLOC1	1.00	1.72	0.76	
AK025872	TNRC8	1.00	1.70	0.70	
U31110	TRPC1	0.91	1.53	0.49	
AW024437	TTC18	0.78	1.16	0.44	
AW779859	UBE2Q1	1.27	1.53	0.73	
AC084239	ZNF228	0.85	1.39	0.57	
AF352582	ABCC11	1.51	1.10	9.85	IFN

Continued

Table 2. Microarray analysis of γ-ray modulation of E_2-dependent genes (*Continued*)

Accession number	Gene name (Symbol)	Fold change (control = 1)			Pathways
		8 Gy	E_2	8 Gy + E_2	
U05598	AKR1C2	0.90	0.91	2.08	PGR/IFN
NM_153042	AOF1	1.00	0.73	1.76	
D90427	AZGP1	0.66	1.05	4.18	ER
U37546	BIRC3	0.84	0.85	2.82	NF-κB
NM_004335	BST2	1.18	1.05	2.69	NF-κB /IFN
AI935123	C14orf78	1.01	0.56	1.33	
AI970144	CACNA2D2	0.97	0.63	1.27	stress
NM_004591	CCL20	1.09	1.20	4.69	NF-κB
NM_022467	CHST8	1.05	0.61	1.29	stress
NM_006536	CLCA2	0.92	1.05	4.97	
AV706254	CTSD	1.91	0.97	4.05	IFN/ER
NM_014314	DDX58	0.78	1.36	5.22	IFN
AI763378	EHF	0.86	0.81	3.03	
AF359241	FGFR4	0.97	0.77	1.64	
NM_001450	FHL2	0.82	0.70	1.82	NF-κB
NM_017631	FLJ20035	0.70	1.20	3.58	
AK023743	FLJ31033	0.56	0.92	1.97	
AI193973	FLJ42461	1.52	0.58	1.82	
NM_001453	FOXC1	1.72	0.75	3.91	
NM_005101	G1P2	0.51	1.14	2.94	IFN
NM_022873	G1P3	1.16	1.78	4.41	IFN/senescence
X61094	GM2A	0.81	0.64	1.56	NF-κB
NM_016295	GP2	1.15	0.74	2.13	
NM_018485	GPR77	1.36	0.61	2.22	
NM_000187	HGD	1.49	1.01	3.62	
NM_005532	IFI27	0.94	1.20	4.12	IFN
NM_001548	IFIT1	0.63	1.46	39.10	IFN
AA131041	IFIT2	0.71	1.88	6.05	IFN
AI075407	IFIT3	1.16	1.38	16.67	IFN
AA749101	IFITM1	0.97	1.07	4.27	IFN/senescence
NM_006084	ISGF3G	0.71	1.04	5.67	IFN
AI074145	KMO	1.88	0.94	6.55	
NM_014583	LMCD1	1.09	1.43	3.47	EMT
R49343	LOC200312	1.30	0.70	2.32	
BF691523	LOC283551	1.00	0.75	1.72	
AA570178	LOC392790	1.01	0.72	1.52	
AL021977	MAFF	1.05	0.75	2.18	
NM_005204	MAP3K8	1.01	0.96	2.18	
AA565509	MGC39606	0.92	0.93	2.38	
AF422798	MLL	1.30	0.75	2.35	
AF274945	NA	1.00	1.26	2.70	
AL049452	NA	1.00	0.33	0.93	
BF439063	NA	0.76	0.96	2.81	
AF228422	NMES1	1.03	0.99	4.10	
NM_002534	OAS1	0.72	1.06	4.46	NF-κB /IFN
NM_016817	OAS2	0.88	0.73	1.85	IFN/senescence
NM_003733	OASL	0.77	0.68	2.05	NF-κB
NM_024607	PPP1R3B	1.31	0.91	3.47	EMT
S78505	PRLR	1.23	0.83	2.08	EMT
AI440266	RDHE2	1.33	1.12	4.26	
AI337069	RSAD2	0.90	1.04	2.42	
NM_002963	S100A7	1.96	0.68	47.70	
NM_002964	S100A8	1.25	1.08	20.35	NF-κB
NM_002965	S100A9	0.68	0.80	3.58	NF-κB/senescence
NM_017654	SAMD9	0.94	1.04	6.96	
NM_002411	SCGB2A2	1.03	0.97	3.51	
NM_000295	SERPINA1	0.64	0.69	5.13	
NM_002639	SERPINB5	0.74	0.74	5.42	NF-κB
NM_020427	SLURP1	1.05	0.70	1.48	
AW015140	ST8SIA6	1.10	0.68	1.71	
BC002704	STAT1	0.89	1.03	2.24	IFN/NF-κB/senescence
AI141151	SYNPO2L	0.91	0.88	4.51	

Continued

Table 2. Microarray analysis of γ-ray modulation of E_2-dependent genes (*Continued*)

Accession number	Gene name (Symbol)	Fold change (control = 1) 8 Gy	E_2	8 Gy + E_2	Pathways
AV726673	THBS1	1.18	1.20	3.05	
AW272342	THRSP	1.51	1.18	7.66	
NM_018004	TMEM45A	1.37	1.20	3.73	
NM_006290	TNFAIP3	1.19	1.25	3.00	NF-κB
U06641	UGT2B15	2.00	1.72	15.53	
AF177272	UGT2B28	1.27	1.07	5.85	
NM_024626	VTCN1	0.62	0.70	1.43	

Abbreviations: EMT = epithelial mesenchyme transition; ER = estrogen-regulated gene; PGR = progesterone-regulated gene; IFN = interferon-associated gene.

induced cell cycle modulators (*CDKN1A* and *GADD45*) or pro-apoptotic gene (*FAS, BAX*) expression, but it did increase expression of p53 and of pro-survival genes (*BIRC5* and *GDF15*). In the absence of p53 regulation, we examined the expression of $p21^{waf1/cip1}$-dependent genes. As previously reported, $p21^{waf1/cip1}$ may support p53-dependent or -independent growth inhibition and senescence (21, 22). $p21^{waf1/cip1}$ modulates genes encode for growth- and senescence-related proteins (23). In the absence or presence of γ-ray treatment, E_2 impeded $p21^{waf1/cip1}$ dependent gene down-regulation (*e.g., TGFβ1, VAV3, MCM2, FEN1, RAD51A, TFF3, MKI67, CENPF, TOP2A*) and $p21^{waf1/cip1}$+-dependent gene expression (*CAV2*, *GRN*) (data not shown). These microarray data suggest that, in IR-cells, E_2 led to an increase in cell proliferation but to a decrease in senescence-modulating p21-dependent gene expression independently of p53 regulation.

We also analyzed the impact of ionizing radiation on E_2 response in BCC (Table 2). No significant modulation of E_2 response was observed for 1,325 probe sets (data not shown). As expected, E_2 increased expression of canonical E_2-targeted genes (*TFF1, PGR, STC2, CXCL12, NRIP1, MYC, TPD52L1*) (24) and modulated growth-associated gene in a sense favorable to cell growth. For instance, expressions of *CCNE2* and *MYC* were increased, whereas expressions of *SKP2* and *CCNG2* were decreased. By contrast, irradiation induced modulation of E_2 response for 132 genes (Table 2). The expression of 62 genes was significantly decreased (more than 2-fold) in IR-cells as compared with non–IR-cells in the presence of E_2. These genes did not appear to be related to any biologic process (as analyzed by Ingenuity Pathways software), but they did seem to be associated with an enhancement of differentiation (*PRLR* or epithelial mesenchyme transition (EMT)–related genes such as *NRF1, ID2B,* and *EFNB3*). On the other hand, simultaneous treatment by irradiation and E_2 specifically increased expression of 70 genes. They were clearly associated with cytokine (interferon and tumor necrosis factor) and/or nuclear factor–κB (NF-κB) responses (25–27). Altogether, these results indicated that irradiation modified E_2 effect on cell differentiation and enhanced E_2 response via NF-κB, which may increase resistance of breast cancer cells to ionizing radiation.

E_2 prevented premature senescence induced by γ-rays

As shown above, E_2 might prevent IR-cells from undergoing senescence. To confirm this hypothesis, premature senescence was assessed by SA–β-galactosidase staining. As shown in Fig. 3, The SA–β-galactosidase activity was increased in IR-cells (45% of cell stain) as compared with non-IR cells (10%). Increase of SA–β-galactosidase activity in MCF-7 cells was only shown 4 days after irradiation and remained constant up to 6 days (data not shown). The E_2 decreased the occurrence of SA–β-galactosidase–positive cells in both non-IR cells and IR-cell cultures, indicating that E_2 effectively precluded premature senescence in MCF-7 BCC.

E_2 prevented Rb dephosphorylation by γ-rays

Many E2F-target genes were down-regulated by γ-rays, whereas E_2 increased expression of these E2F targets in IR-cells (Table 1). It is possible that E2F activity is suppressed by binding to the dephosphorylated form of Rb protein. Phosphorylation of Rb allows dissociation of E2F, thereby permitting the induction of cell cycle genes (28). We hypothesized that the effects of γ-rays and E_2 on E2F were mediated by Rb; thus the level and phosphorylation status of Rb were evaluated by immuno-blotting (Fig. 4a).

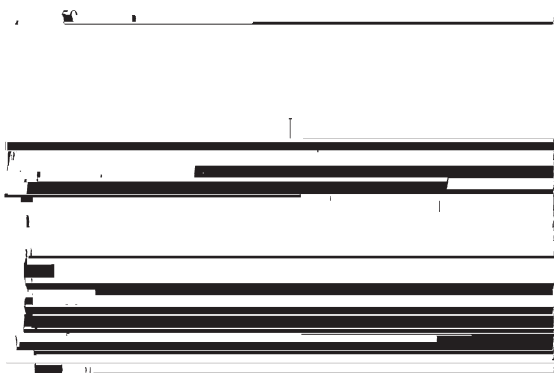

Fig. 3. Effects of E_2 on IR-cells senescence. Senescence induction was measured by SA–β-gal staining 96 h after 8-Gy γ-ray exposure. Results are representative of three independent experiments performed in triplicate.

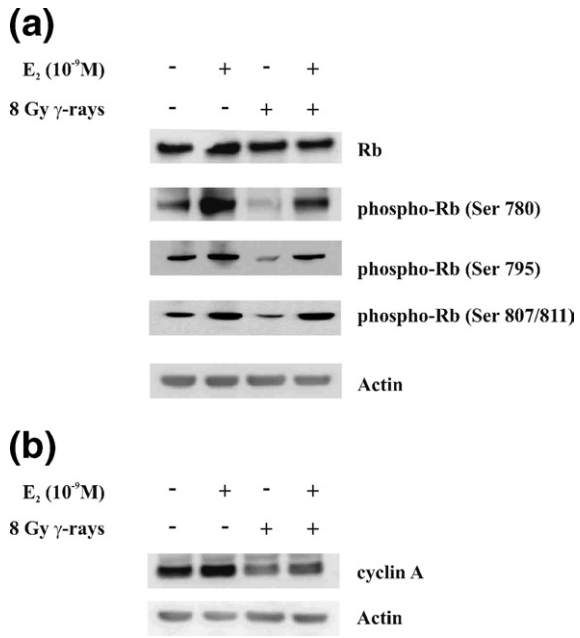

Fig. 4. Effects of E_2 on Rb regulation in irradiated breast cancer cells (IR-cells). (a) Total Rb expression, Rb protein phosphorylation status, and (b) levels of cyclin A, an E2F-dependent cell cycle protein, were assessed by western blot 24 h after 8-Gy γ-ray exposure. Proteins 25 μg for Rb and phospho-Rb; 50 μg for cyclin A were electrophoresed and western blot analysis performed as described in Methods and Materials. Loading and transfer of equal amounts of protein were confirmed by immunodetection of actin. Data shown are representative of three separate experiments.

No modification of Rb level was observed after γ-rays and/or E_2 treatments; Rb phosphorylation on several serine residues (780, 795 and 807/811) was then assessed. In non–IR-cells, E_2 increased Rb phosphorylation on Ser 780 and in a lesser extent on Ser 795 and Ser 807/811. On all serine residues 8-Gy γ-rays decreased Rb phosphorylation, an effect that was impeded by E_2. Because *CCNA2* is a well-known E2F target gene, we measured its product, cyclin A, by an immunoblotting technique (Fig. 4b). We found that E_2 slightly increased cyclin A level in non–IR-cells and sustained its expression in IR-cells, further supporting E2F activation.

E_2 induced dissociation of p21$^{waf1/cip1}$/cyclin E2 complexes independently of p53 regulation in IR cells

p53 activity was checked by immunoblotting (Fig. 5a), and treatment with γ-rays was found to increase p53 level. This increase followed a biphasic kinetic. Such complex kinetic was previously reported and attributed to the activation of the p53-associated MDM2 ubiquitin ligase (29). In IR-cells, E_2 did not prevent an increase in p53 level or its biphasic activation. The p53 activity, evaluated by its ability to bind its consensus DNA sequence, was then examined by DuoSet IC active p53 ELISA kit (Fig. 5b). Nuclear extracts from IR-cells exhibited an increase in p53 binding to the consensus sequence as compared with non–IR-cells. Treatment with E_2 did not modify the increase of p53 binding in IR-cells. p21$^{waf1/cip1}$ is known to play an essential role in p53-dependent and -independent cell cycle arrest and senescence (30). The p21$^{waf1/cip1}$ level was then determined by western blotting; as shown in Figure 5c, the p21$^{waf1/cip1}$ level was increased in IR-cells. We found that E_2 did not block p21$^{waf1/cip1}$ induction in IR-cells. In the absence of p21$^{waf1/cip1}$ modulation, we also analyzed other CDK inhibitors such as p16^{ink4a} and p27^{kip1}. As previously described, we did not observe p16^{ink4a} expression in MCF-7 cells (31) (data not shown). Expression of p27^{kip1} was also assessed

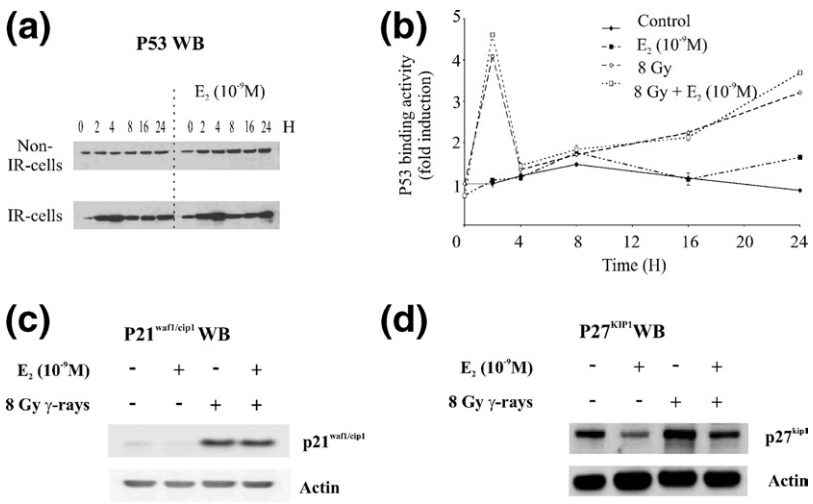

Fig. 5. Modulation of p21$^{waf1/cip1}$ by E_2 is independent of p53 in irradiated breast cancer cells (IR-cells). p53 levels were assessed by western blotting (a), and p53 activation was appreciated by its ability to bind consensus sequence (b) in 8-Gy γ-ray IR-cells up to 24 h. Western blot analysis of p21$^{waf1/cip1}$ (c) and p27^{kip1} in MCF-7 BCC (d). Proteins (25 μg) were electrophoresed and Western blots performed as described in Methods and Materials. Loading and transfer of equal amounts of protein were confirmed by immunodetection of actin. Results were representative of three independent experiments (a, c) and of two independent experiments (b, d) performed in triplicate.

by western blot (Fig. 5d). In non-IR cells, immunoblot analysis showed that E_2 decreased $p27^{kip1}$ basal expression. Moreover, E_2 prevented a γ-ray exposure–induced increase in $p27^{kip1}$ expression, which remained at the basal rate.

It has been shown previously that under E_2 stimulation, increased levels of cyclin D1/cdk4 associate to $p21^{waf1/cip1}$, which leads to the concomitant decrease in $p21^{waf1/cip1}$/cyclin E2/cdk2 complexes. Dissociated cyclin E2/cdk2 is activated and phosphorylates Rb (31, 32). To confirm such a hypothesis, $p21^{waf1/cip1}$ binding to cyclin D1 and E_2 were appreciated by immunoprecipitation. As shown in Fig. 6, E_2 did not significantly enhance cyclin D1 association with $p21^{waf/cip1}$ (Fig 6a), whereas it decreased $p21^{waf/cip1}$ binding to cyclin E_2 (Fig 6b). Altogether, these results suggest that E_2 decreased cyclin E2/$p21^{waf1/cip1}$ complexes in IR-cells.

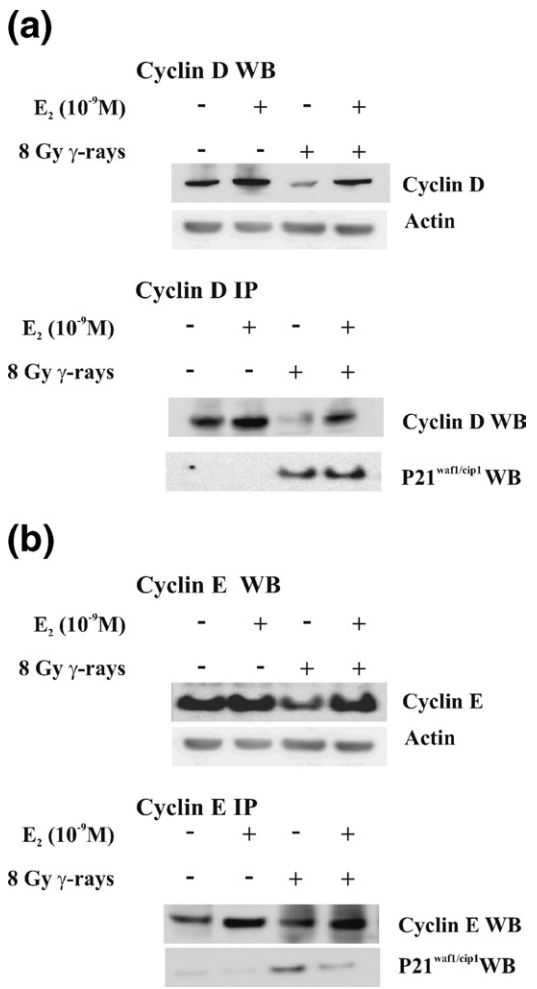

Fig. 6. E_2 induced redistribution of $p21^{waf1/cip1}$ from cyclin D1 to cyclin 2. At 24 h after γ-ray exposure, 1 mg of total cell extract was subjected to immunoprecipitation by a rabbit anti-cyclin D1 (a) or anti-cyclin E_2 (b) antibody and was followed by anti-cyclin D1 or anti-cyclin E_2 and anti-$p21^{waf1/cip1}$ immunoblots. As a control, 50 μg of total cell extract were also electrophoresed and Western blots for cyclin D1 and E_2 performed as described in Methods and Materials. Loading and transfer of equal amounts of protein were confirmed by immunodetection of actin. Results were representative of two (a) or three (b) independent experiments.

DISCUSSION

The present study shows that E_2 may partly prevent the BCC growth arrest induced by low γ-ray doses (<8 Gy), increasing clonogenic survival of BCC. At higher γ-ray doses, E_2 still sustained cell proliferation but no longer enhanced clonogenicity (data not shown). Moreover, we observed that E_2 prevented senescence in both non–IR-cells and IR-cells. Altogether, our data suggest that low γ-ray doses induce cell growth arrest through senescence that may be prevented by E_2. Higher γ-ray doses induce growth arrest through senescence and other mechanisms that may reflect harmful genetic lesions.

According to our microarray data, E_2 modulated IR-induced p53/$p21^{waf1/cip1}$/Rb pathways. Activation of p53 is known to result in a complex response in IR-cells. It seems insufficient to trigger apoptosis, but it induces a temporary (cell cycle arrest) or prolonged (senescence) cell growth arrest, and DNA repair (33). Interestingly, ERα expression in luminal breast cancer is rarely associated with mutation in *Tp53*, the p53 gene. Because most *Tp53* mutations lead to a p53 loss-of-function (34), this suggests that estrogen action on BCC mainly bypass p53 inhibitory effects. Accordingly, Molinari *et al.* (11) reported that E_2 stimulation may inactivate p53 through nuclear export. In agreement with a recent study (35), our data suggest that E_2 bypasses p53 growth inhibitory effects by acting on p53 downstream targets.

Under our conditions, E_2 did not inhibit p53 activation; but the hormone acted downstream p53, redistributing $p21^{waf1/cip1}$ from cyclin E_2 complexes. As a consequence of its effect on $p21^{waf1/cip1}$, E_2 prevented the dephosphorylation of Rb, an event that is known to mediate γ-ray–induced cell cycle arrest (36). Indeed, the hypophosphorylated Rb binds to members of the E2F transcription factor family and thereby antagonizes their ability to up-regulate genes involved in cell cycle progression and DNA repair (37). The hypophosphorylated Rb may also trigger senescence. Based on our data, it is thus likely that Rb inactivation and E2F activation may be responsible for the E_2 effects on cell growth, senescence, and radio-resistance.

Numerous reports indicate that DNA damage contributes to cellular senescence (21–23, 33, 38, 39). Senescence is associated with SA–β-galactosidase staining and is characterized by the expression of both growth inhibitor and paracrine tumor promoting factors. Two pathways have been implicated in the induction of cellular senescence involving p53 or $p16^{ink4a}$. In absence of $p16^{ink4a}$ expression in our MCF-7 BCC (data not shown), we have focused our investigation on p53-induced senescence. Nevertheless, we have shown that E_2 blocks senescence by disrupting $p21^{waf1/cip1}$ activation and not p53 in IR-cells. More precisely, E_2 treatment does not affect p53-dependent growth-regulated gene expression (*GADD45A, BAX, FAS*), whereas it increases p53-dependent growth-promoting factor (*GDF15, BIRC5*). These observations are consistent with a recent study demonstrating that p53 is involved in the cell growth arrest and

senescence just after γ-ray exposure, but that it acts as a protective factor that allows population recovery (33). Interestingly, our results indicated that E_2 may enhance this p53-protective effect. On the other hand, E_2 functionally targets $p21^{waf1/cip1}$, a downstream effector of p53. Based on our data, it appears that this effect of E_2 may be caused by the decrease in $p21^{waf1/cip1}$-dependent gene expression but also by $p21^{waf1/cip1}$/cyclin E complex dissociation. This effect of E_2 on $p21^{waf1/cip1}$ may explain the decrease in senescence. Nevertheless, we observed that E_2 also affects basal senescence induction in MCF-7 BCC in the absence of irradiation. These results emphasize the fact that $p21^{waf1/cip1}$ potentially enhanced senescence but was not necessary to trigger it. In these conditions, we suggest that senescence is probably linked to pRb phosphorylation status. Nevertheless, we cannot exclude E2F/pRb-independent effects of cyclin E on other substrates that may involve in DNA maintenance (40). Definitely, E_2 may both alter cdk-inhibitors expression ($p21^{waf1/cip1}$, $p15^{ink2b}$, $p27^{kip1}$) or activity ($p21^{waf1/cip1}$) and enhance cyclin expression (cyclin D, E, A) or activation (cyclin E). Altogether these effects of E_2 converge to increase pRb phosphorylation and its inhibition.

The effects of E_2 on radiosensitivity of BCC lines may also provide a rationale for the concomitant use of endocrine therapies and radiotherapy. Although endocrine therapies may affect the survival potential of IR-cells, clinical evidence of agonist vs. antagonist effects of tamoxifen endocrine therapy are still discussed (41). By contrast, concomitant anti-aromatase therapy seems to act synergistically (42). This discrepancy may reflect the complexity of the tamoxifen response in BCC. Indeed, tamoxifen is a selective estrogen receptor modulator which may act as an estrogen receptor antagonist but also as an agonist, depending of the cell context. This property may be the basis for the frequent appearance of tamoxifen resistance in BCC. Interestingly, irradiation induced a dramatic change in estrogen receptor-mediated response corresponding to an enhancement of NF-κB and/or interferon response (*BST2, IFI27, IFIT1, OAS1, OAS3, STAT1*); these genes are normally down-regulated by estrogen and up-regulated by inhibitors such as tamoxifen or aromatase inhibitors (43). Recently, Biswas *et al.* (44) have suggested that reactivation of NF-κB may contribute to hormone resistance of BCC. In addition, NF-κB induction is frequently associated with cancer cell resistance to radiation (45), chemotherapy (46), and apoptosis (47).

Our investigations have been performed *in vitro*. One cannot exclude the possibility that the BCC response *in vivo* could be different because of variations in factors relating to treatment (*e.g.,* dose, sequence, time lapse). Physiologic mechanisms such as repopulation and senescence induction might also be underestimated *in vitro*. Moreover, it is likely that the microenvironment of BCC *in vitro* may modulate the tumor responsiveness to radiotherapy and endocrine therapy. These modulations might result from bystander effects (48), direct ionizing radiation effects on neighboring normal cells such as fibroblasts (49), and complex integration of multiple autocrine, paracrine, or hormone-stimulated pathways (50, 51).

CONCLUSION

In conclusion, our studies showed that E_2 induced cell cycle regulators that sustained radioresistance of BCC and radiotherapy modified estrogen response in favor of cancer cell resistance. However, further studies are required to dissect physiologic mechanisms triggered by the hormone to provide a better understanding of the complex interactions between E_2 and $p53/p21^{waf1/cip1}$/Rb pathway and of the interference between hormone and adjuvant therapies (*i.e.,* endocrine, chemo-, and radiotherapies).

REFERENCES

1. Lacroix M, Toillon RA, Leclercq G. Stable 'portrait' of breast tumors during progression: Data from biology, pathology and genetics. *Endocr Relat Cancer* 2004;11:497–522.
2. Shaaban AM, O'Neill PA, Davies MP, *et al.* Declining estrogen receptor-beta expression defines malignant progression of human breast neoplasia. *Am J Surg Pathol* 2003;27:1502–1512.
3. Bardin A, Boulle N, Lazennec G, *et al.* Loss of ERbeta expression as a common step in estrogen-dependent tumor progression. *Endocr Relat Cancer* 2004;11:537–551.
4. Bjornstrom L, Sjoberg M. Mechanisms of estrogen receptor signaling: Convergence of genomic and nongenomic actions on target genes. *Mol Endocrinol* 2005;19:833–842.
5. Schmidberger H, Hermann RM, Hess CF, *et al.* Interactions between radiation and endocrine therapy in breast cancer. *Endocr Relat Cancer* 2003;10:375–388.
6. Toillon RA, Magne N, Laïos I, *et al.* Interaction between estrogen receptor alpha, ionizing radiation and (anti-) estrogens in breast cancer cells. *Breast Cancer Res Treat* 2005;93: 207–215.
7. Zhang Z, Kumar R, Santen RJ, *et al.* The role of adapter protein Shc in estrogen non-genomic action. *Steroids* 2004; 69:523–529.
8. Zhou Y, Eppenberger-Castori S, Eppenberger U, *et al.* The NFκB pathway and endocrine-resistant breast cancer. *Endocr Relat Cancer* 2005;12:S37–S46.
9. Kim IA, Bae SS, Fernandes A, *et al.* Selective inhibition of Ras, phosphoinositide 3 kinase, and Akt isoforms increases the radiosensitivity of human carcinoma cell lines. *Cancer Res* 2005;65:7902–7910.
10. Ikeda K, Inoue S. Estrogen receptors and their downstream targets in cancer. *Arch Histol Cytol* 2004;67:435–442.
11. Molinari AM, Bontempo P, Schiavone EM, *et al.* Estradiol induces functional inactivation of p53 by intracellular redistribution. *Cancer Res* 2000;60:2594–2597.
12. Lacroix M, Leclercq G. Relevance of breast cancer cell lines as models for breast tumours: An update. *Breast Cancer Res Treat* 2004;83:249–289.
13. Toillon RA, Chopin V, Jouy N, *et al.* Normal breast epithelial cells induce p53-dependent apoptosis and p53-independent cell cycle arrest of breast cancer cells. *Breast Cancer Res Treat* 2002;71:269–280.
14. Dimri GP, Lee X, Basile G, *et al.* A biomarker that identifies senescent human cells in culture and in aging skin *in vivo. Proc Natl Acad Sci USA* 1995;92:9363–9367.

15. Irizarry RA, Bolstad BM, Collin F, *et al.* Summaries of Affymetrix GeneChip probe level data. *Nucleic Acids Res* 2003;31:e15.
16. Jen K, Cheung V. Identification of novel p53 target genes in ionizing radiation response. *Cancer Res* 2005;65:7666–7673.
17. Zhang H, Pan KH, Cohen SN. Senescence-specific gene expression fingerprints reveal cell-type-dependent physical clustering of up-regulated chromosomal loci. *Proc Natl Acad Sci USA* 2003;100:3251–3256.
18. Xin H, Pereira-Smith OM, Choubey D. Role of IFI 16 in cellular senescence of human fibroblasts. *Oncogene* 2004;23: 6209–6217.
19. Collado M, Gil J, Efeyan A, *et al.* Tumour biology: Senescence in premalignant tumours. *Nature* 2005;436:642.
20. Fridlyand J, Snijders AM, Ylstra B, *et al.* Breast tumor copy number aberration phenotypes and genomic instability. *BMC Cancer* 2006;6:96.
21. Elmore LW, Di X, Dumur C, *et al.* Evasion of a single-step, chemotherapy-induced senescence in breast cancer cells: Implications for treatment response. *Clin Cancer Res* 2005;11: 2637–2643.
22. Chen Y, Dokmanovic M, Stein WD, *et al.* Agonist and antagonist of retinoic acid receptors cause similar changes in gene expression and induce senescence-like growth arrest in MCF-7 breast carcinoma cells. *Cancer Res* 2006; 66:8749–8761.
23. Chang BD, Swift ME, Shen M, *et al.* Molecular determinants of terminal growth arrest induced in tumor cells by a chemotherapeutic agent. *Proc Natl Acad Sci USA* 2002;99:389–394.
24. Creighton CJ, Cordero KE, Larios JM, *et al.* Genes regulated by estrogen in breast tumor cells *in vitro* are similarly regulated *in vivo* in tumor xenografts and human breast tumors. *Genome Biol* 2006;7:R28.
25. Der SD, Zhou A, Williams BR, Silverman RH. Identification of genes differentially regulated by interferon alpha, beta, or gamma using oligonucleotide arrays. *Proc Natl Acad Sci USA* 1998;95:15623–15628.
26. Banno T, Gazel A, Blumenberg M. Pathway-specific profiling identifies the NF-kappa B-dependent tumor necrosis factor alpha-regulated genes in epidermal keratinocytes. *J Biol Chem* 2005;280:18973–18980.
27. Einav U, Tabach Y, Getz G, *et al.* Gene expression analysis reveals a strong signature of an interferon-induced pathway in childhood lymphoblastic leukemia as well as in breast and ovarian cancer. *Oncogene* 2005;24:6367–6375.
28. Frolov MV, Dyson NJ. Molecular mechanisms of E2F-dependent activation and pRB-mediated repression. *J Cell Sci* 2004; 117:2173–2181.
29. Ma L, Wagner J, Rice JJ, *et al.* A plausible model for the digital response of p53 to DNA damage. *Proc Natl Acad Sci USA* 2005;102:14266–14271.
30. Larsson O. Cellular senescence-an integrated perspective. *Cancer Ther* 2005;3:495–510.
31. Foster SJ, Henley DC, Bukovsky A, *et al.* Multifaceted regulation of cell cycle progression by estrogen: Regulation of cdk inhibitors and cdc25A independent of cyclin D1-cdk4 function. *Mol Cell Biol* 2001;21:794–810.
32. Planas-Silva MD, Weinberg RA. Estrogen-dependent cyclin E-cdk2 activation through p21 redistribution. *Mol Cell Biol* 1997;17:4059–4069.
33. Jones KR, Elmore LW, Jackson-Cook C, *et al.* p53-Dependent accelerated senescence induced by ionizing radiation in breast tumour cells. *Int J Radiat Biol* 2005;81:445–458.
34. Lacroix M, Toillon RA, Leclercq G. p53 and breast cancer, an update. *Endocr Relat Cancer* 2006;13:293–325.
35. Boulay F, Perdiz D. 17Beta-estradiol modulates UVB-induced cellular responses in estrogen receptors positive human breast cancer cells. *J Photochem Photobiol B* 2005;81:143–153.
36. Harrington EA, Bruce JL, Harlow E, *et al.* pRB plays an essential role in cell cycle arrest induced by DNA damage. *Proc Natl Acad Sci USA* 1998;95:11945–11950.
37. Bracken AP, Ciro M, Cocito A, *et al.* E2F target genes: Unraveling the biology. *Trends Biochem Sci* 2004;29:409–417.
38. Roninson IB. Tumor cell senescence in cancer treatment. *Cancer Res* 2003;63:2705–2715.
39. te Poele RH, Okorokov AL, Jardine L, *et al.* DNA damage is able to induce senescence in tumor cells in vitro and in vivo. *Cancer Res* 2002;62:1876–1883.
40. Ye X, Wei Y, Nalepa G, Harper JW. The cyclin E/Cdk2 substrate p220(NPAT) is required for S-phase entry, histone gene expression, and Cajal body maintenance in human somatic cells. *Mol Cell Biol* 2003;23:8586–8600.
41. Schmidberger H, Hermann RM, Hess CF, *et al.* Combination of anti-estrogenic therapy with radiation in breast cancer: Simultaneous or sequential treatment? *Onkologie* 2005;28: 275–280.
42. Azria D, Larbouret C, Cunat S, *et al.* Letrozole sensitizes breast cancer cells to ionizing radiation. *Breast Cancer Res* 2005;7:R156–R163.
43. Itoh T, Karlsberg K, Kijima I, *et al.* Letrozole-, anastrozole-, and tamoxifen-responsive genes in MCF-7aro cells: A microarray approach. *Mol Cancer Res* 2005;3:203–218.
44. Biswas DK, Singh S, Shi Q, Pardee AB, Iglehart JD. Crossroads of estrogen receptor and NF-kappaB signaling. *Sci STKE* 2005;288:pe27.
45. Magne N, Toillon RA, Bottero V, *et al.* NF-kappaB modulation and ionizing radiation: Mechanisms and future directions for cancer treatment. *Cancer Lett* 2006;231:158–168.
46. Montagut C, Tusquets I, Ferrer B, *et al.* Activation of nuclear factor-κB is linked to resistance to neoadjuvant chemotherapy in breast cancer patients. *Endocr Relat Cancer* 2006;13:607–616.
47. Toillon RA, Descamps S, Adriaenssens E, *et al.* Normal breast epithelial cells induce apoptosis of breast cancer cells via Fas signaling. *Exp Cell Res* 2002;275:31–43.
48. Prise KM, Schettino G, Folkard M, *et al.* New insight on cell death from radiation exposure. *Lancet Oncol* 2005;6:520–528.
49. Tsai KK, Chuang EY, Little JB, *et al.* Cellular mechanisms for low-dose ionizing radiation-induced perturbation of the breast tissue microenvironment. *Cancer Res* 2005;65:6734–6744.
50. Becker KA, Lu S, Dickinson ES, *et al.* Estrogen and progesterone regulate radiation-induced p53 activity in mammary epithelium through TGF-beta-dependent pathways. *Oncogene* 2005;24:6345–6353.
51. Vares G, Ory K, Lectard B, *et al.* Progesterone prevents radiation-induced apoptosis in breast cancer cells. *Oncogene* 2004;23:4603–4613.